SF2A 2024
M. Béthermin, K. Baillié, N. Lagarde, J. Malzac, R.-M. Ouazzani, J. Richard, O. Venot, A. Siebert (eds)

3D EXTINCTION MAPPING OF THE MILKY WAY WITH THE BESANÇON GALAXY MODEL IN THE GAIA ERA

B. Déforêt[1], J. Montillaud[1], A. C. Robin[1] and D. J. Marshall[2]

Abstract. 3D extinction maps are important tools to study the structure of our Galaxy. They offer a view of the Milky Way at different scales, from spiral arms down to molecular clouds. Since the release of precise parallax measurements with *Gaia* DR3, the precision of 3D extinction maps increased, but not their spatial coverage. In this paper, we present a method to produce 3D extinction maps that extend to large distances with a reasonable spatial resolution. We detail the basis of our method and apply it to the region of Vela C and Orion for validation. We show that our method is able to use 2MASS and *Gaia* data without cross-match to determine dust distribution at large distances. Our method being still in development, we present possible ameliorations and perspectives for the future of this work.

Keywords: Galaxy, structure, ISM, dust, extinction

1 Introduction

The structure of the Milky Way (MW) disc remains poorly constrained in spite of numerous studies. The challenge comes from the fact that we are inside the MW disc, which makes all structures overlap along the line of sight (LOS), so that the global structure of our Galaxy is still debated. Hou & Han (2014) used HII regions, Giant molecular clouds and maser distances to show that the MW could either have three or four spiral arms. Reid et al. (2019) uses maser distances from the BeSSeL survey to propose a model with four logarithmic spiral arms. Xu et al. (2023) used masers, massive O-B2 type stars and open cluster parallaxes and showed that data are compatible with a symmetric two-arm model.

3D extinction maps aim to characterize the distribution of dust within our Galaxy. They allow studying both large scale, like spiral arms, and small scale structures, like molecular clouds, as long as their resolution and spatial coverage is sufficient. Recent studies (Chen et al. 2019; Green et al. 2019; Leike et al. 2022; Lallement et al. 2022), usually provide detailed 3D extinction maps, but that only extend to a few kiloparsecs or that only covers the very local Galactic disc. More importantly, they often rely on data obtained from the cross-match of different surveys, limiting their distance range to the survey that is most affected by extinction.

In this paper, we present a new method, PyRedLine, to map the distribution of dust within the MW in 3D, based on observational data and the Besançon Galaxy Model (BGM, Robin et al. 2003; Czekaj et al. 2014; Lagarde et al. 2017; Robin et al. 2022), a stellar population synthesis model that simulates the stellar content of the MW. This model is a tool to constrain evolutionary scenarios of the MW, or to constrain the Galactic structure, such as dust distribution, by comparing model predictions to observations. Our method uses multiple surveys without cross-match, in order to map the dust distribution in the MW at large distances while keeping a reasonable amount of details. We use *Gaia* DR3 photometric data and parallaxes, as well as 2MASS photometric data for Vela C and Orion regions to test the method. We briefly describe the advantages and current limitations of our method, as well as the ongoing work and some perspectives for its future.

[1] Université de Franche-Comté, CNRS UMR6213, Institut UTINAM, OSU THETA Franche-Comté-Bourgogne, Observatoire de Besançon, BP 1615, 25010 Besançon Cedex, France
[2] IRAP, Université de Toulouse, CNRS, UPS, CNES, 9 Av. colonel Roche, BP 44346, 31028 Toulouse Cedex 4, France

2 Data

The Two Micron All Sky Survey (2MASS) is a ground based survey that made uniformly-calibrated observations of the entire sky in the three near infrared bands J (1.25 μm), H (1.66 μm) and K_s (2.16 μm). We used photometric data from the 2MASS point source catalogue (PSC) by selecting sources with photometric errors below 0.5 mag. The completeness of the sample is determined by taking the maximum of the magnitude distribution for the sample. This distribution is obtained by evaluating a Gaussian kernel on the magnitude count histogram, in order to smooth the distribution. In addition, we add strict limits to our selection, such that $9 \leq J \leq 16.1$ mag, $9 \leq H \leq 15.5$ mag and $9 \leq K_s \leq 15.1$ mag.

The *Gaia* space mission observes the entire sky in the visible domain. Its third Data Release (DR3) contains parallaxes and photometric measurements in G_{BP} (511 nm), G (621 nm) and G_{RP} (776 nm) for about 1.5 billion sources. We used *Gaia* DR3 photometric data and parallaxes by selecting sources with measurements for all the three bands and parallax. The completeness of the sample is computed using the same method as for 2MASS data. For *Gaia*, strict limits to our selection are $5 \leq G_{BP} \leq 20$ mag, $5 \leq G \leq 20$ mag and $5 \leq G_{RP} \leq 20$ mag.

As already mentioned, the extinction effect increases with shorter wavelengths, making *Gaia* unable to observe stars at large distances, unlike 2MASS. We combined 2MASS and *Gaia* data without cross-match, offering us the possibility to benefit from the advantages of each survey, i.e. high precision at short distances with *Gaia* and information at large distances with 2MASS.

3 PyRedLine

3.1 Single LOS estimation

Our method, PyRedLine, is an evolution of Redline, a 3D extinction mapping technique developed by Marshall et al. (in prep.). RedLine was used to map the entire Galactic plane for $|b| < 1$ using only 2MASS photometry. PyRedLine is able to use both 2MASS and *Gaia* Photometry, as well as *Gaia* parallaxes, in order to better constrain the 3D dust distribution in the MW. It is based on the assumption that the differences between the BGM-predicted and observed stellar distributions are solely due to extinction.

For a given LOS, the problem is parametrized by a set of N differential extinction value $\{\delta A_i\}_{i=1}^N$ arranged onto a regularly spaced distance grid. The total amount of extinction at a given distance r_n is then given by:

$$A(r_n) = \sum_{i=1}^{n} \delta A_i \delta r \tag{3.1}$$

where δr is the distance step and $n \in [1, N]$. The posterior probability function of model parameter $\{\delta A_i\}_{i=1}^N$ given observations O is given by Bayes Theorem:

$$P\left(\{\delta A_i\}_{i=1}^N | O\right) \propto P\left(O | \{\delta A_i\}_{i=1}^N\right) P\left(\{\delta A_i\}_{i=1}^N\right) \tag{3.2}$$

The comparison between model and observation is done in two ways: (i) via colour histograms, only based on 2MASS and *Gaia* photometry and (ii) via parallax-colour histograms, based on *Gaia* photometry and astrometry only. Following Bienayme et al. (1987), if we assume that the distribution of stars in each histogram bin j follows a Poisson distribution, the log-likelihood of observing O stars given that the model predicts M stars is:

$$P\left(O | \{\delta A_i\}_{i=1}^N\right) = \sum_j O_j \left[1 - \frac{M_j(\{\delta A_i\}_{i=1}^N)}{O_j} + \ln\left(\frac{M_j(\{\delta A_i\}_{i=1}^N)}{O_j}\right)\right] \tag{3.3}$$

The prior consists in penalising solutions that give negative differential extinction, or that give a total extinction that is above a maximum value. The penalities grow as the exponential of the difference between the actual value and the limits. The posterior distribution is explored by a Monte Carlo Markov Chain (MCMC) to estimate the most probable dust distribution along a LOS so that the colour distribution of observation and model stars are in agreement. We used emcee (Foreman-Mackey et al. 2013) for the MCMC implementation. The parameter space was explored with 10 times more walkers than parameters and for a total of 12000 steps. The median, 16^{th} and 84^{th} percentiles for the last 100 steps are used for the best estimate, as well as the lower and upper uncertainties for each parameter, respectively. The Fitzpatrick et al. (2019) extinction law is used to convert from A_0 (extinction at 541.4 nm) to the extinction at the effective wavelength of each band of each survey. This law is parametrized by the total to selective extinction ratio R_V set to 3.1.

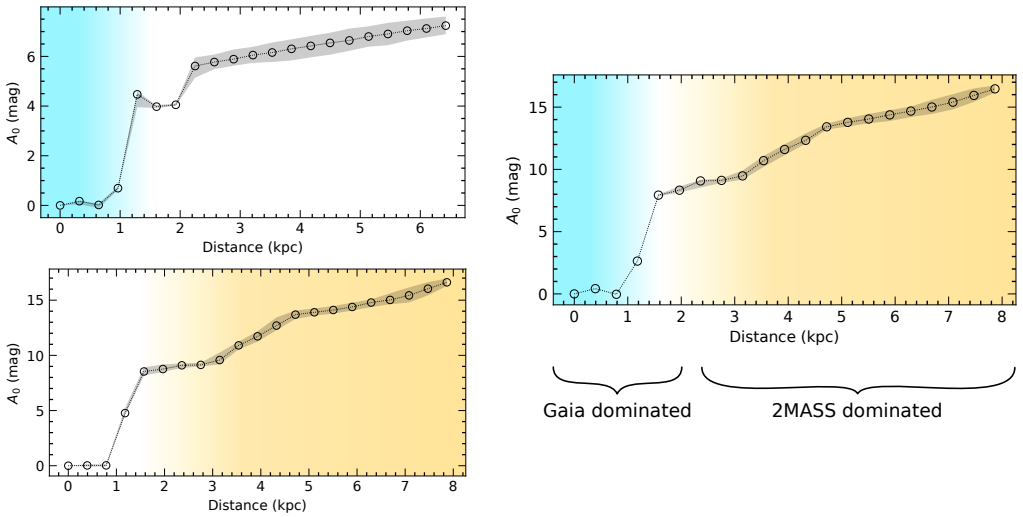

Fig. 1. Single extinction profiles in the direction of Vela C, at $l = 266.1°$, $b = 1°$. **Top-left:** fit obtained using *Gaia* data only. **Bottom-left:** fit obtained using 2MASS data only. **Right:** fit obtained using a combination of *Gaia* and 2MASS data. The gray shaded region corresponds to the uncertainty at 1σ. The cyan and yellow parts highlight the distance range where each survey provides the most information when using them together.

We applied this method to the Vela C molecular cloud, located at ∼917 pc (Zucker et al. 2020). Figure 1 shows extinction profiles obtained for a single LOS through Vela C (l,b = 266.1, 1.0 deg), with a 30' field of view. We compared the results when using *Gaia* data alone, or 2MASS data alone, or their combination. A structure is identified between 0.8 and 1.4 kpc, a distance compatible with Vela C. The figure emphasizes the distance range that is best constrained by each survey (cyan shaded region for *Gaia*, yellow for 2MASS), showing that the combination of both survey, without cross-match, is effective.

3.2 3D mapping

Our method allows us to estimate an extinction profile for any LOS. It is then possible to estimate the extinction profile for concurrent LOS in order to obtain a 3D extinction map. We tested our method in the Orion region. Integrated extinction maps for the region of Orion (Fig. 2) show a good agreement between the structures that can be identified in the Planck space telescope dust opacity map and those visible in the integrated extinction map obtained with PyRedLine. This agreement is also good when comparing our map with Lallement et al. (2022) integrated extinction map (hereafter denoted L22). The correlation between them is strong, even if some regions of our map seem to have higher extinction values than in the L22 map for $A_0 > 1.5$ mag.

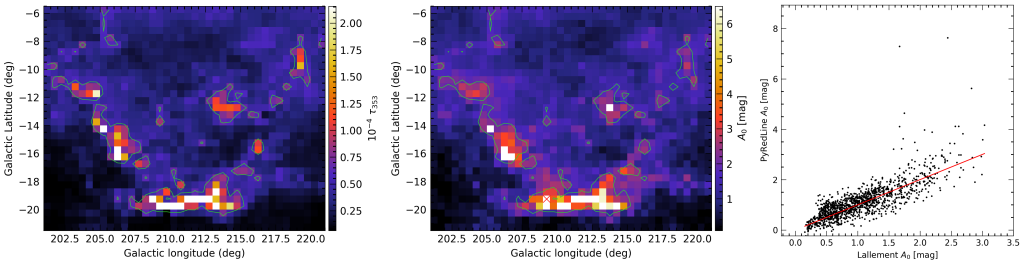

Fig. 2. Left: Planck dust opacity map. **Middle:** PyRedLine integrated extinction map. **Right:** correlation between PyRedLine and L22 integrated extinction maps. Green contours corresponds to Planck $\tau_{353} = 6.0 \times 10^{-5}$. The red line represents the perfect correlation. The red cross denotes a LOS where the method failed to estimate the extinction profile.

Presently, PyRedLine is unable to detect Orion's location, at ∼ 400 pc (Zucker et al. 2020). While L22 finds a structure around 400 pc with a size of ∼ 50 pc, we find an elongated structure that spans an entire kiloparsec.

This inaccurate finding shows that some improvements are still necessary to our method. The stellar density in Orion is lower than the density within the Galactic plane. Having less stars per LOS can degrade the results. Furthermore, Orion is a star forming region. It contains local overdensities of young stars that the BGM does not model, thus potentially leading to erroneous results.

4 Ongoing work and perspectives

The spatial resolution of our extinction profile is defined by the number of points and the distance range covered by the profile. We used only 20 points to cover 5 kpc. We thus have a resolution of 250 pc and the first kiloparsec is covered by only 4 points. This is a coarse resolution, and improving it should help to better resolve identifiable structures. In addition, we plan to consider the fractal structure of the ISM by modelling it with a log-normal probability density function. Furthermore, for each pixel on the map, the method considers that the dust distribution is homogeneous over the plane of the sky. However, dust column density gradients within a pixel impact the stellar colour distribution, which can lead to untrustworthy results.

Our method is strongly bound to the BGM. We plan to assess the sensitivity of our results to the parameters, assumptions, and usage method of this model. Our method has not been tested extensively on regions within the Galactic plane. We plan to map the entire MW for $|b| \leq 1°$. We will then be able to compare our results with other maps, such as the maps from Marshall et al. (in prep.) and Cornu et al. (2022) that also use the BGM as a reference.

5 Conclusions

We presented PyRedLine, a 3D extinction mapping technique that can estimate the dust distribution along any line of sight in the Milky Way. Thanks to the use of the BGM, we are not bound to data with parallax measurement. Furthermore, we can combine multiple surveys without cross-match, allowing us to benefit from the advantages of each survey. We tested our method in Vela C and Orion. While the method is very effective at retrieving the position of Vela C for a single LOS, as well as the overall 2D dust distribution of Orion, it fails to find the location of Orion. Multiple improvements are under study and the final method will soon be presented in Déforêt et al. (in prep.).

This publication makes use of data products from the Two Micron All Sky Survey, which is a joint project of the University of Massachusetts and the Infrared Processing and Analysis Center/California Institute of Technology, funded by the National Aeronautics and Space Administration and the National Science Foundation. This work has made use of data from the European Space Agency (ESA) mission *Gaia* (`https://www.cosmos.esa.int/gaia`), processed by the *Gaia* Data Processing and Analysis Consortium (DPAC, `https://www.cosmos.esa.int/web/gaia/dpac/consortium`). Funding for the DPAC has been provided by national institutions, in particular the institutions participating in the *Gaia* Multilateral Agreement.

References

Bienayme, O., Robin, A. C., & Crézé, M. 1987, A&A, 180, 94
Chen, B.-Q., Huang, Y., Yuan, H.-B., et al. 2019, MNRAS, 483, 4277–4289
Cornu, D., Montillaud, J., Marshall, D. J., Robin, A. C., & Cambrésy, L. 2022, arXiv
Czekaj, M. A., Robin, A. C., Figueras, F., Luri, X., & Haywood, M. 2014, A&A, 564, A102
Fitzpatrick, E. L., Massa, D., Gordon, K. D., Bohlin, R., & Clayton, G. C. 2019, ApJ, 886, 108
Foreman-Mackey, D., Hogg, D. W., Lang, D., & Goodman, J. 2013, PASP, 125, 306–312
Green, G. M., Schlafly, E., Zucker, C., Speagle, J. S., & Finkbeiner, D. 2019, ApJ, 887, 93
Hou, L. G. & Han, J. L. 2014, A&A, 569, A125
Lagarde, N., Robin, A. C., Reylé, C., & Nasello, G. 2017, A&A, 601, A27
Lallement, R., Vergely, J. L., Babusiaux, C., & Cox, N. L. J. 2022, A&A, 661, A147
Leike, R. H., Edenhofer, G., Knollmüller, J., et al. 2022, arXiv
Marshall, D. J., Montillaud, J., Cambrésy, L., & Cornu, D. in prep.
Reid, M. J., Menten, K. M., Brunthaler, A., et al. 2019, ApJ, 885, 131
Robin, A. C., Bienaymé, O., Salomon, J. B., et al. 2022, A&A, 667, A98
Robin, A. C., Reylé, C., Derrière, S., & Picaud, S. 2003, A&A, 409, 523–540
Xu, Y., Hao, C. J., Liu, D. J., et al. 2023, ApJ, 947, 54
Zucker, C., Speagle, J. S., Schlafly, E. F., et al. 2020, A&A, 633, A51